Article:
Nottingham, AT orcid.org/0000-0001-9421-8972, Scott, JJ, Saltonstall, K et al. (5 more authors) (2022) Microbial diversity declines in warmed tropical soil and respiration rise exceed predictions as communities adapt. Nature Microbiology, 7 (10). pp. 1650-1660. ISSN 2058-5276

https://doi.org/10.1038/s41564-022-01200-1

Microbial diversity decline and community response are decoupled from increased respiration in warmed tropical forest soil

Andrew T. Nottingham[1,2,3*], Jarrod J. Scott[3], Kristin Saltonstall[3], Kirk Broders[3,4], Maria Montero-Sanchez[3], Johann Püspök[3], Erland Bååth[5], Patrick Meir[2,6]

Affiliations:

[1]*School of Geography, University of Leeds, Leeds, UK*

[2]*School of Geosciences, University of Edinburgh, Crew Building, Kings Buildings, Edinburgh, UK*

[3]*Smithsonian Tropical Research Institute, 0843-03092, Balboa, Ancon, Republic of Panama*

[4]*USDA, Agricultural Research Service, National Center for Agricultural Utilization Research, Mycotoxin Prevention and Applied Microbiology Research Unit. Peoria, IL. 61604, USA*

[5]*Section of Microbial Ecology, Department of Biology, Lund University, 22362, Lund, Sweden.*

[6]*Research School of Biology, Australian National University, Canberra, ACT 2601, Australia*

**Corresponding author. Email: A.Nottingham@leeds.ac.uk*

Perturbation of soil microbial communities by rising temperatures could have important consequences for biodiversity and future climate, particularly in tropical forests where high biological diversity coincides with a vast store of soil carbon. We carried out a two-year *in situ* soil warming experiment in a tropical forest in Panama and found large changes in the soil microbial community and its growth sensitivity, which did not fully explain observed large increases in CO_2 emission. Microbial diversity, especially of bacteria, declined markedly with 3 to 8°C warming, demonstrating a breakdown in the positive temperature-diversity relationship previously observed in temperate-zones. The microbial community composition shifted with warming, with many taxa no longer detected and others enriched, including thermophilic taxa. This community shift resulted in community-adaptation of bacterial growth to warmer temperatures, which we used to predict changes in soil CO_2 emissions. However, the *in situ* CO_2 emissions exceeded our model predictions three-fold, likely driven by abiotic acceleration of enzymatic activity. Our results suggest that warming of tropical forests will have rapid, detrimental consequences both for soil microbial biodiversity and future climate.

MAIN

Microbial communities sustain the biosphere by cycling carbon (C) and nutrients between the Earth and the atmosphere. As a result, their response to warming provides a fundamental feedback on the terrestrial C cycle and climate, and will have direct consequences for the function and maintenance of terrestrial biota[1]. The nature of this feedback is especially critical for tropical forests, because they exchange more carbon dioxide (CO_2) with the atmosphere than any other ecosystem, contain over a third of global soil C[2], two-thirds of terrestrial plant biomass[3], and represent the apex of global terrestrial biodiversity[4]. Under current emission scenarios, temperatures in the tropics are predicted to warm by 2-5°C by 2100[5] and to exceed historical precedent more quickly than anywhere else on Earth[6]. Despite this, we have almost no information on the magnitude and direction of soil microbial feedbacks under warming for the huge C stores and biodiversity found in tropical forests[7].

Climate warming is predicted to increase the mineralization of soil organic matter and, consequently, the emission of CO_2 from soil to the atmosphere[8]. Numerous experiments performed outside the tropics have shown that warming increases CO_2 emission from soil[9], and that changes in the activity and community composition of soil microbes influence the associated soil C loss[10,11]. In tropical forests where soils contribute a major portion of these ecosystems' globally significant total C exchange with the atmosphere[12], small fractional increases in CO_2 emission from soils will have a large impact on the atmosphere and climate. Warming experiments in tropical forests have only recently been initiated and first results point towards a large response. Two years of *in situ* full-profile soil warming by an average 4°C increased the soil CO_2 efflux by 55% for a tropical forest in Panama[13]. This result provokes key fundamental questions: what are the drivers of the large CO_2 emissions from warmed tropical forest soils – and are they related to abiotic or biotic processes, including changes in

the composition of the microbial community, its diversity and/or its activity, as found in other ecosystems[10,11,14].

The response of soil C to warming is underpinned by changes in soil microbial activity, via the instantaneous sensitivity of microbial growth and respiration, which can be modified over time by adaptive change in the microbial community composition[10,15]. These microbial responses have been represented in models of soil C temperature sensitivity by the efficiency of growth and respiration[16], while the thermal response of growth and respiration has been described by the square root model[15,17]. In the square root model, the moderating effect of temperature adaptation is described by a change in the theoretical value of T_{min} (the minimum temperature for growth), corroborated by observations that T_{min} is strongly correlated to mean annual temperature differences across climatic gradients globally[18-20]. For example, T_{min} for bacterial growth ranges from approximately -15°C in arctic ecosystems to approximately 0°C for tropical ecosystems, with similar patterns observed for T_{opt}[15,19] and for respiration[20]. Across temperate temperature ranges, T_{min} has been observed to increase under experimental warming[21,22] alongside community compositional shifts[14,23,24], thus indicating that the observed thermal adaptation occurred via microbial community composition change. Despite the proven importance of this relationship in determining the temperature response of activity and its thermal adaptation[15,17], we have no information on whether it holds under warming in the lowland tropics, where the mean annual temperature is already close to the predicted optima for metabolic activity[15].

The effect of warming on tropical forest soil C will depend not only on the response of the soil microbial community activity[7], but also its community composition and diversity, which may have consequences for other biota[25]. In a temperate forest, two decades of experimental warming increased bacterial diversity,[14] specifically for lignin-degrading microbes[26]; this positive temperature-diversity

106 relationship is consistent with observations across natural temperature gradients where soil pH and
107 moisture are held constant[23,27,28]. It is unknown whether soil microbial diversity will similarly increase
108 under the novel high-temperature regimes predicted for the tropics[6] and will depend on the thermal
109 tolerance of the microbial taxa present[24,29]. Nor is it understood how diversity change would affect soil
110 process rates, although the effect might be considerable given phylogenetic evidence for high niche
111 specialization among tropical forest microbial taxa[30]. The historically-novel high temperature regimes
112 predicted for the tropics this century[6] (e.g. 2-5°C atmospheric warming[5] added to 1-3°C warming
113 through land-use change and reduced transpiration[31]) could result in temperature maxima that exceed
114 a metabolic threshold for portions of the tropical forest soil microbial community, with potentially
115 large implications for ecosystem functioning and the climate.
116
117 Here we used an *in situ* warming experiment to test the response of the soil microbial community, and
118 its growth and respiration to warming over a range of 3 to 8°C above ambient – thereby providing a
119 test of how tropical forest soil communities and function respond across these levels of warming in a
120 field experiment. The experiment, SWELTR (Soil Warming Experiment in Lowland TRopical forest)
121 consists of five pairs of circular control and warmed plots (whole-profile warming, using buried
122 resistance cables) distributed evenly within approximately 1 ha of semi-deciduous moist lowland
123 tropical forest on Barro Colorado Island, Panama[13]. Each warmed plot has a ground surface area of
124 ~20 m^2 and is heated across the full soil profile, resulting in a total of 120 m^3 of warmed soil for the
125 experiment (Extended Data Fig. 1). For this study we established two subplots per treatment plot that
126 differed with distance to the heating source, thus providing two treatments of, on average, 3°C and 8°C
127 warming of surface soils (0–20 cm depth). Two years after the warming treatment was initiated, we
128 conducted field campaigns during the wet season (when moisture was non-limiting) to measure soil
129 CO_2 efflux, to characterise the temperature sensitivity of instantaneous microbial growth, respiration
130 and enzyme activities, and to determine the microbial community composition. We tested the

hypotheses that: (1) warming will change the α-diversity and community composition of soil bacteria and fungi; (2) the temperature sensitivity of microbial communities (with respect to growth, T_{min}, and enzymatic activity) will become 'adapted' to the new temperature regime (whether adaptation is via genetic change within species, phenotypic plasticity or community-composition change, *sensu* Pietikäinen et al.; Bradford [32,33]); and (3) soil CO_2 emission will increase under 3 to 8°C warming and follow the increase predicted by the temperature sensitivity of microbial growth and respiration.

RESULTS

Microbial diversity

Two years of soil warming reduced the diversity of both bacteria and fungi and caused large shifts in the microbial community composition (Fig. 1). The diversity decline was largest for bacteria, occurring via the loss of proportionally-abundant taxa (Shannon and Inverse-Simpson indices declined; Fig. 1, Extended Data Fig. 2). For fungi, our results suggest a diversity decline due to loss of rare taxa (species richness declined but not Shannon and Inverse-Simpson indices), although this result is less definitive than for bacteria, given methodological issues influencing the detection of rare taxa (see Supplementary Methods) and our identification of different fungal taxa in warmed soils (see below). Warmed soils also hosted microbial species (defined by Amplicon Sequence Variants, ASVs) that were undetected in soils at ambient temperature, especially among fungi, although the number of newly detected species was too few to offset the number of species no longer detected (Fig. 1). This decline in diversity, especially for the bacteria, may have implications for soil functioning, given the prevailing paradigm of a positive relationship between biological diversity and ecosystem functioning[34], also supported for soils[35,36]. Such a decline in soil microbial diversity under warming is also contrary to positive relationships between temperature and diversity observed in a temperate warming experiment[14] and across natural environmental gradients[27,28,37]. This positive relationship is consistent with metabolic theory of ecology (i.e. positive correlation between energy input,

156 evolutionary rates and diversity)[38] and is considered to be one of several positive feedbacks on tropical
157 plant diversity[39-41]. Our results point towards a breakdown in this energy-diversity relationship for
158 tropical soil bacterial communities after a two-year period where temperatures ranged from 29–34°C.
159 These temperatures may represent a thermal maximum for the persistence of many species, implying
160 that our findings can also provide insight over timescales longer than the duration of our warming
161 treatment.
162
163 **Microbial community composition**
164 Warming also caused large shifts in community composition (Figs. 1–2, Extended Data Figs. 2–5),
165 with many taxa significantly increasing or decreasing in relative abundance with warming by 3°C, and
166 further with warming by 8°C (Fig. 1; Extended Data Figs. 3–4). In warmed soils there was a decrease
167 in the relative abundance of Bacteroidetes, a common non-spore-forming bacterial group which
168 comprise taxa that are primary degraders of polysaccharides[42]. For fungi, there was decrease in the
169 relative abundance of members of the Basidiomycota including the Agaricales, a broad order of
170 saprophytic and ectomycorrhizal fungi, and the ecologically diverse yeast order, Sporidiobolales. In
171 contrast, warming increased the relative abundance of Firmicutes, a diverse and stress-tolerant
172 bacterial phylum, able to form endospores resistant to desiccation and high temperatures[43]. Indeed,
173 taxa within the Firmicutes have been identified as warm-responsive in laboratory studies[24,29] and in
174 field soil warming experiments outside the tropics[14,44]. Warming also increased the abundance of the
175 class Thermoleophilia within the Actinobacteria, known to include aerobic thermophiles[45]. For fungi,
176 warming increased the relative abundance of Glomerales—arbuscular mycorrhizae—as also seen in
177 warming experiments outside the tropics[46]. In addition, warming increased the relative abundance of
178 several orders in the phylum Ascomycota, including the Eurotiales, Hypocreales and Pezizales, which
179 include thermotolerant saprophytic and pathogenic species, as well as saprophytic and pathogenic

yeast in the Saccharomycetales. Thus, broadly, changes in diversity under warming occurred alongside shifts in communities towards thermotolerant microorganisms.

Growth adaptation to temperature

Adaptation of the microbial community to warming potentially can have a large influence on long-term change in soil C emissions[10,16]. To assess this, we used laboratory incubations to determine the instantaneous temperature sensitivity of bacterial growth (T_{min}) following the square root model[15,17], whereby changes in T_{min} reflect a community-adaptation to temperature, a response empirically related to shifts in the community composition[24]. In the square root model, the effect of temperature on activity is described by a quadratic increase up to an optimal temperature ($T_{opt,}$) and then a sharp decline[15,17], where the quadratic phase of the increase is constrained by the minimum temperature for activity (T_{min}, the y-intercept of the square root of activity plotted against temperature), which is higher for microbial communities adapted to warmer temperatures[15]. Following two years of experimental warming at our tropical forest site, we found T_{min} to increase under 3°C warming and to increase further under 8°C warming (Fig. 2); where the observed magnitude of increase in T_{min}, of 0.3°C per 1°C warming, is consistent with observations made elsewhere[15]. Furthermore, among all the parameters associated with temperature adaptation in the field experiment, T_{min} was the most significant correlate of the change in bacterial and fungal diversity and community composition (Fig. 2e, Extended Data Tables 1–2). Thus, while acknowledging that we cannot exclude an influence of genetic change within species on this temperature adaptation, our results strongly suggest that adaptation occurred through community compositional change, as found elsewhere[24], and the development of a microbial community functionally adapted to the warmer conditions.

Soil process rates

The changes in diversity and community composition occurred alongside altered soil process rates in the field experiment: increased bacterial growth rates, enzyme activity per unit microbial biomass for 7 hydrolytic and oxidative enzymes involved in C, N and P cycling (although microbial biomass remained stable) and, measured *in situ*, increased soil CO_2 emission (Figs. 2–3, Extended Data Figs. 6–7). Soil CO_2 emission in the field experiment increased markedly at warmer temperatures: 78% higher than controls under 3°C warming and 337% higher under 8°C warming of surface soils (Fig. 3; Extended Data Table 3). The soil CO_2 efflux response for the wet season was consistent with the previously-reported 55% increase over 2-years of 3°C surface soil warming at this experiment (including dry and wet seasons), which was shown to have arisen predominantly from increased heterotrophic microbial activity[13]. Our observation of increased soil metabolic activity, indicated by increased bacterial growth and enzyme activity with *in situ* soil warming, describes a further acceleration of heterotrophic activity with warming. Enzymatic activity per unit of microbial biomass increased for 7 out of 10 studied enzymes and markedly at +8°C *in situ* warming for enzymes that degrade organic phosphorus, nitrogen, and carbon in phenolic and hemicellulose compounds (Fig. 2, Extended Data Fig. 6–7). Collectively, the observed changes in process rates—of increased respiration, growth and enzymatic activity per unit microbial biomass—corroborate our parallel findings that the microbial community shifted towards favouring thermotolerant taxa that readily persist and even increase in productivity under warmer conditions.

Predicted and observed soil CO_2 emission under warming

We used the instantaneous temperature sensitivity of bacterial growth (T_{min}) to model the CO_2 efflux response to warming, both with (T_{min} determined for soil from warmed treatments) and without (T_{min} determined for soil from controls) microbial community temperature adaptation. Here we used T_{min} for bacteria growth only, because there was no significant difference in the T_{min} for bacterial growth (-1.4 ± 0.8) and respiration (0.3 ± 0.4) in control soils (P = 0.1). The T_{min} values for bacterial

229 growth in control soils were also similar to those determined independently for two lowland tropical
230 forests in Peru with similar mean annual temperature (-1.66 ± 0.7, -1.77 ± 1.0; MAT = 26.4°C)[19]. To
231 model the CO_2 efflux response to warming following temperature-adaptation of microbial
232 communities, we refitted the Ratkowsky model (see methods) using the T_{min} determined for bacterial
233 growth in experimentally warmed soils for two years by 3°C and 8°C ('adapted' communities).

234 The predicted increase in soil CO_2 efflux based on the measured temperature sensitivity of
235 microbial respiration and growth in control soils (24–68% increase under 3–8°C warming; Fig. 3), was
236 substantially exceeded by the observed *in situ* increase in soil CO_2 efflux (78–337% under 3–8°C
237 warming; Fig. 3). Furthermore, the predicted CO_2 emission was only marginally higher when
238 accounting for adaptation of the microbial community to warmer conditions (measured T_{min} increase;
239 Fig. 2), resulting in a 25–77% increase under 3–8°C warming (Fig. 3). Importantly, we found no
240 evidence to suggest that the observed *in situ* increase in soil CO_2 emission occurred due to decreased
241 microbial metabolic efficiency, a common finding in short-term soil warming experiments where high
242 waste respiration exceeds growth[47]. Reduced metabolic efficiency is inconsistent with our previously
243 reported observation of no decrease in the size of the microbial biomass or in microbial carbon use
244 efficiency[48] (measured using a stoichiometric method, see Methods for discussion of this method and
245 its assumptions; Extended Data Fig. 6); a result in line with the independent observation of increased
246 microbial biomass under soil warming in tropical forest in Puerto Rico[49]. Similarly, we cannot explain
247 the augmented soil CO_2 emission by reference to accelerated substrate depletion or substrate depletion
248 alongside priming effects where microbes acquire additional N or P from organic sources[50], which
249 would also be expected to cause an eventual decline in microbial biomass[48,51]. On the contrary, we
250 found no change in microbial biomass despite evidence for substrate depletion (decreased DOC and
251 available P at 8°C warming; Extended Data Fig. 6).

252 Soil warming can also induce soil drying, potentially influencing CO_2 emission and other
253 community and process rate changes[8]. However, our study here was focused on the tropical rainy

season and despite lower moisture content in our +8°C treatment (Extended Data Fig. 6), we expect this had negligible influence on our results because moisture remained non-limiting to microbial activity. Finally, the augmented *in situ* soil CO_2 emission cannot be explained by increased root respiration or substrate supply from root exudates, because by using root-partitioning cores we found that warming had no effect on the root-derived soil CO_2 efflux[13]. Thus, we show that the temperature response of microbial community metabolism to warming—considered in models to be fundamental in explaining the long-term, and relatively large, response of soil C to climate warming[16,48]—only accounted for 23–32% of the observed *in situ* soil CO_2 emission.

Abiotic processes may increase CO_2 emissions

In addition to biotic processes, our data point towards a further influence of abiotic processes in accelerating CO_2 emission at warmer temperatures. By using *ex situ* soil incubations across 2–40°C, we found that microbial growth declined at temperatures exceeding 34°C (Fig. 2); but enzyme activities measured under both *ex situ* and *in situ* warming increased—as did *in situ* soil CO_2 emissions (Figs. 2–3; Extended Data Figs. 6-7). These results can be explained by the effect of warming on the soil physico-chemical environment, including chemical oxidation/hydrolysis and desorption of mineral-stabilised organic matter and extracellular enzymes[52]. Clay-rich soils, such as those found at our tropical forest site, contain a large pool of stabilised C and inactive extracellular enzymes adsorbed to clay minerals.[53] At high temperatures desorption reaction rates can overtake adsorption reaction rates[54], thereby increasing the pools of active enzymes and labile C, and consequent CO_2 emissions. Independent observations support this mechanism of an abiotic contribution to enzyme activity under warming: of high respiration and enzymatic activity in sterilised soils[55,56], and of stable enzyme functioning at high temperatures[57]. Consistent with a rapid increase in the pool of active enzymes driven by desorption, under warming we observed increased Q_{10} of V_{max} for four enzymes including phosphomonoesterase, β-xylanase and β-glucosidase (Fig. 2, Extended Data Fig. 6). This is counter to

279 the prediction of reduced Q_{10} for 'warm-adapted' iso-enzymes thought to result from increased folding
280 and decreased flexibility[54,58] but it is consistent with a rapid increase in the pool of active enzymes
281 under warming, driven by desorption reactions[59].

282 Enhanced soil CO_2 emissions driven by accelerated enzyme activities under warming could
283 also occur through chemical oxidation. Under aerobic conditions, oxides of Fe and Mg minerals—
284 abundant in many tropical soils including at our study site—provide electron acceptors that catalyse
285 the degradation of phenol compounds and the formation of reactive organic compounds[56,60]. Because
286 we focused on responses during the wet season when moisture was non-limiting, soil drying at higher
287 levels of warming may have increased O_2 supply, increasing the activity of oxidative enzymes and
288 organic matter oxidation[56,60,61]. Consistent with this mechanism, soil moisture declined at 8°C
289 (although not to the extent to cause moisture limitation; Extended Data Figure 6) alongside a marked
290 increase in the activity of phenol oxidase (Extended Data Table 3). It is therefore likely that a
291 combination of these processes resulted in increased enzyme activity that was uncoupled from growth
292 (Fig. 2), contributing substantially to the observed CO_2 emissions that exceeded the predicted increase
293 based on standard expectations from the observed temperature sensitivity and warm-adaptation
294 response of the microbial community[15] (i.e. it was exceeded by 3.1–4.4 fold; Fig. 3).

295

296 **DISCUSSION**

297 In summary, our results show a progressive decline in tropical forest soil microbial diversity, especially
298 for bacteria, and clear microbial community compositional shifts with warming (Fig. 1), occurring
299 alongside community growth-adaptation to temperature (Fig. 2) and resulting in further increased CO_2
300 emission (Fig. 3). This response of diversity declines under warming is contrary to observations from
301 temperate forest warming studies[14,26]. Our data thus provide empirical support for the hypothesis that
302 tropical soil communities are highly sensitive to warming and are consistent with independent
303 evidence for deep evolutionary niche specialization in tropical soil microbes[30]. Further, we note that

in view of the widespread evidence for intensive feedbacks among tropical soil microbial communities, plant diversity, and soil processes[25,41,62], declines in diversity may have substantial implications for the resilience of tropical forest functioning, composition, and diversity in a warmer world. Alongside the decline in diversity observed in this experiment, the concurrent increased abundance of thermotolerant species resulted in a stable microbial biomass, accelerated enzymatic activity, and increased soil CO_2 emissions. This finding partially supports prior model-based projections showing increased C loss under climate warming this century due to adaptation of microbial growth[16]. However, our results go further by demonstrating that microbial models alone do not accurately predict the change in soil C emissions under warming in tropical ecosystems, especially at high temperatures where abiotic processes may accelerate C loss. Further study is urgently required to understand these combined biotic and abiotic controls on soil C in different tropical soils and land-use contexts, the timescales of their effects, and the wider consequences of declines in soil microbial diversity for the functioning and composition of tropical forests in a warmer world.

METHODS

Site and experiment. The experiment is situated in seasonally moist lowland tropical forest on Barro Colorado Island, Panama. Within the experiment area (1 ha) the dominant tree species include *Anarcardium excelsum* and *Poulsenia armata;* a full census of tree and understory species composition in this forest is available for a nearby 50 ha forest plot in forest with similar soils, tree species and demographic composition[63]. The soils are Inceptisols (Fine, isohyperthermic, Dystric Eutrudepts) that are rich in clay (~54% profile-weighted clay concentration) and secondary metal oxides. The soils developed on the volcanic facies of the Bohio Formation, a basaltic conglomerate of Oligocene age[64]. Inceptisols account for 14% of total land area in the tropics (Ultisols and Oxisols account for 20% and 23%, respectively)[65].

The SWELTR experiment consists of 10 circular plots (five paired plots 'warm' and 'control'). Each plot measures 5 m diameter, with approximately 10 m between each plot-pair and a minimum of 20 m between different plot-pairs. The experiment heats approximately 120 m^3 soil in total (5 plots x 5 m diameter by 1.2 m depth). Temperature in the internal plot area (~3 m diameter) of each warmed plot was maintained at 4°C above the temperature in each corresponding paired control plot, based on the average temperature from 0–120 cm depth at the mid-radius points in each plot. For this study we established subplots representing a high-temperature treatment, situated in a buffer-zone close to the heating cable. We therefore had two subplots per plot, situated at approximately 10 cm and 1 m distance from the one of the main heating rods, representing two different levels of warming. The average warming for the low-warming subplot was 2.8°C and for the high-warming subplot was 7.9°C (determined at 0–10 cm soil depth), based on the difference in temperature between control plots. Thus, our study consisted of three treatments, soil at 26 ± 1°C ('Control'), 29 ± 2°C ('+3°C') and 34 ± 7°C ('+8°C'), providing a test of moderate (atmospheric warming with moderate fossil fuel emission reduction) to extreme (atmospheric warming plus deforestation) predictions of warming for tropical soils this century[5,31]. Further information on the plot design, thermostat control and power specifications can be found in Nottingham *et al.* 2020[13].

Soil gas-exchange and partitioning. Soil CO_2 efflux was measured every week at four systematically distributed locations within each plot from June 2018 to September 2018 (representing the 3°C surface soil-warming treatment); and was measured twice-weekly at two systematically distributed locations within the high-warming subplot from August to September 2018 (representing the 8°C surface soil-warming treatment). Soil CO_2 efflux measurements were made using an infra-red gas analyser (IRGA Li-8100; LI-COR Biosciences, Nebraska, USA) and at the same time we measured soil temperature (using a HI98509 thermometer probe; Hanna Instruments, USA) and soil moisture (using a

354 Thetaprobe; Delta-T, Cambridge, UK) at 0–20 cm soil depth for a random location immediately
355 adjacent to each soil collar.
356
357 ***Soil sampling.*** Soil for this study was sampled during the wet season (June–Sept) in 2018. We sampled
358 during the wet season to ensure that there was no moisture limitation to soil microbial activity and soil
359 processes, and no difference in moisture limitation among treatments. Soil was sampled from 0–10 cm
360 depth from the mineral horizon for each subplot and analysed for properties: total elements, available
361 nutrients, exchangeable cations, microbial C, N and P and enzyme activities using standard procedures
362 (see below). We calculated microbial carbon-use-efficiency (CUE) using microbial C, N and P and
363 enzyme activity data using a stoichiometric method (see below). All analyses were determined on
364 fresh soils within 24 hours of sampling, except for K_2SO_4 extracts on fresh soils within 6 h; growth
365 assays on fresh soils within ~14 days; total elements (C, N, P), cations, and pH on air-dried soil
366 samples; and samples for microbial community analyses stored at −60°C until DNA extraction. All
367 analyses were performed on replicate soil samples (n = 5).
368
369 ***DNA extraction, sequencing, and processing.*** DNA was extracted using the DNeasy Powersoil kit
370 (Qiagen) and communities (bacterial and fungal) were amplified using a two-stage PCR protocol. For
371 bacteria, we amplified the V4 hypervariable region of the 16S rRNA and for fungi we amplified the
372 first internal transcribed spacer (ITS1) region of the rRNA operon (see SI methods for complete
373 details). Libraries were sequenced on an Illumina MiSeq with 250bp paired end reads. Reads in the
374 16S rRNA and ITS data sets were first trimmed of forward and reverse primers. Based on visual
375 inspection of read quality profiles, we removed the reverse reads from the 16S rRNA analysis due to
376 poor quality. We then used DADA2[66] within the R environment (R Core Team, 2019) (v4.1.0) to filter
377 and trim both datasets (based on quality profiles), error correct, dereplicate, and infer amplicon
378 sequence variants (ASVs). We then merged pair-end reads (ITS only) and constructed sequence tables

for both datasets. In the final step, we removed chimeras and assigned taxonomy. For a detailed description of filtering of sequencing data and workflow, including all references, see Supplementary Methods.

Soil properties. Soil microbial biomass C and N were measured by fumigation-extraction[67,68] and extractable C and N were determined by fresh soil extraction in 0.5 M K_2SO_4. Extracts were analyzed for extractable organic C and N using a TOC-VCHN analyzer (Shimadzu, Columbia, MD). Microbial C and N were calculated as the difference between fumigated and unfumigated extracts and corrected for unrecovered biomass using a k factor of 0.45[69]. Microbial biomass P was determined by hexanol fumigation and extraction with anion-exchange membranes[70]. Extractable P was determined using unfumigated samples and microbial P was calculated as the difference between the fumigated and unfumigated samples, with correction for unrecovered biomass using a k_p factor of 0.4[70]. Exchangeable cations were determined by extraction in 0.1 M $BaCl_2$ and detection by inductively coupled plasma-optical emission spectrometry (Optima 7300 DV; Perkin-Elmer Ltd, Shelton, CT, USA). Effective cation exchange capacity (ECEC) was calculated as the sum of the charge equivalents of Al, Ca, Fe, K, Mg, Mn and Na. Soil pH was determined in deionized water in a 1:2 soil to solution ratio. All soil chemical properties are expressed on the basis of oven-dry equivalent soil (determined by drying at 105°C for 24 hours).

Soil enzymes. We determined maximum potential enzyme activity (V_{max}) and the temperature sensitivity of enzyme activity (Q_{10} of V_{max}) for ten enzymes involved in C, N, P and S cycling. We determined V_{max} and Q_{10} of V_{max} for all treatments for in situ warmed soils (control, +3°C, +8°C). For the determination of Q_{10} of V_{max} we determined V_{max} for a range of temperatures using laboratory assays.

Enzymes involved in C cycling under study were: α-glucosidase and β-glucosidase (act on α- and β- bonds in glucose, respectively), cellobiohydrolase (acts on cellulose), β-xylanase (acts on hemicellulose) and phenol oxidase (acts on phenolic compounds). Enzymes involved in P-cycling: phosphomonoesterase and phospho-diesterase (acts on monoester- and diester- linked simple organic phosphates, respectively). Enzymes involved in N-cycling: *N*-acetyl β-glucosaminidase (acts on *N*-glycosidic bonds) and leucine aminopeptidase (acts on amino acid leucine from proteins). Enzyme involved in S-cycling: sulfatase (acts on sulfated glucosamines). For subsequent discussion, enzymes are abbreviated to: α-glucosidase (AG_{ase}), β-glucosidase (BG_{ase}), phosphodiesterase (BP_{ase}), cellolbiohydrolase (CE_{ase}), leucine aminopeptidase (LP_{ase}), phosphomonoesterase (P_{ase}), *N*-acetyl β-glucosaminidase (N_{ase}), phenol oxidase (PX_{ase}), sulfatase (S_{ase}) and β-xylanase (XY_{ase}).

Hydrolytic enzymes (AG_{ase}, BG_{ase}, BP_{ase}, CE_{ase}, P_{ase}, N_{ase}, S_{ase}, XY_{ase}), were measured using microplate fluorometric assays with methylumbelliferone (MU)-linked substrates, except for LP_{ase}, which was measured using L-leucine-AMC substrate (Sigma Aldrich, St. Louis, USA). PX_{ase} was measured using L-dihydroxyphenyalanine (L-DOPA) as substrate (Sigma Aldrich, St. Louis, USA). Fluorimetric substrates were dissolved in 0.4% methylcellosolve (2-methoxyethanol; 0.1% final concentration in the assay). The hydrolytic fluorometric and LP_{ase} methods are based on the protocols described in Tabatabai [71] and Marx, et al. [72]; while the PX_{ase} method is described in Sanchez-Julia and Turner [56].

For each soil sample, five replicate micro-plates were prepared and incubated at 2, 10, 22, 30 and 40°C. For the fluorometric assays, 2 g fresh soil (field moist weight basis) was added to 200 ml of 1mM sodium azide (NaN_3) solution and dispersed by stirring vigorously on a magnetic stir plate. After 5 min, and while stirring, 50 µl aliquots of soil suspension were removed using an 8-channel pipette and dispensed into a 96-well microplate containing 50 µl modified universal buffer solution adjusted to soil pH. Each microplate included assay wells (soil solution, buffer and 100 µl of 200 µM MU substrate; 100 µM MU substrate in final solution), blank wells (soil solution, buffer and 100 µl of

1mM NaN_3) and quench wells (soil solution, buffer and 100 µl MU standard). For LP_{ase}, we used 1mM L-leucine-AMC substrate. There were eight analytical replicate wells for each assay, and control plates for each set of assays with the standards and no soil solution (to determine fluorescence from substrates and quenching by soil solution in assay plates). Microplates were incubated at each specified temperature for 1 to 4 h, with incubation times based on preliminary assays for each specific substrate to assess the linearity of the reaction over time. Following incubation, 50 µl of 0.5 M NaOH was added to each well for MU substrates (but not for AMC substrates) and plates were immediately analyzed on a Fluostar Optima spectrofluorometer (BMG Labtech, Offenburg, Germany) with excitation at 360 nm and emission at 450 nm. For PX_{ase} assays, 1g soil (oven-dry basis) was added to 100 ml of 5 mM bicarbonate buffer and stirred vigorously; 100 µl of 5 mM L-DOPA solution and 100 µl of soil solution were dispensed into a 96-well microplate. Control plates were made using 100 µl of 5mM bicarbonate buffer and 100 µl aliquots of soil solution. There were 16 analytical replicates and controls per soil sample. Plates were analyzed on a spectrofluorometer, with PX_{ase} activity calculated as the increase in absorbance at 450 nm over 1 h. Enzyme activities were expressed on the basis of soil organic C. Hydrolytic enzyme activities, determined using MU substrates, were expressed in nmol substrate (MU or AMC) min^{-1} g C^{-1}. PX_{ase}, determined using L-DOPA as a substrate, was expressed in mg diqc h^{-1} g C^{-1} (where diqc is the L-DOPA product 3-dihydroindole-5,6-quinone-2-carboxylate).

We determined the temperature sensitivity of maximum potential enzyme activity (V_{max}) by calculating Q_{10} values as follows:

$$Q_{10} = exp(10\ x\ k),\ \textbf{where}\ k = ln\frac{V_{max}}{t}\ (equation\ 3)$$

Where k is the exponential rate at which V_{max} increases with temperature (t)[54]. To calculate k (and thus Q_{10}) we used linear regression and included enzyme data determined between 2°C and 40°C. We only determined Q_{10} values of enzyme activity during the exponential increase in activity with temperature according to Arrhenius kinetics, prior to reaching any thermal optima of activity at which dynamics

depart from Arrhenius kinetics. The thermal optima of enzymes are widely associated with enzyme denaturation that begins to occur at temperatures above 40°C [73].

Determination of carbon use efficiency.

Changes in microbial community function, including growth and CUE, has been shown by models to have an extremely large influence on the soil-atmospheric C exchange and soil C storage under climatic change[16,48]. However, empirical evidence on the long-term response of microbial community physiology and its influence on soil C storage is lacking, both in part due to a lack of long-term experimentation and in part due to methodological difficulties in quantifying the relevant microbial community response. Microbial CUE, for example, is an emergent property representing the ratio of C lost in respiration against C accumulated during growth[74] and can be quantified in numerous ways, including using substrate-induced respiration (^{13}C substrates)[75]; ^{18}O labeling in water[76]; mass-balance and the stoichiometry of enzyme activity and biomass[77]. Because it is an emergent property and therefore challenging to quantify, CUE estimates can vary among methods and thus require interpretation with consideration of method used for its quantification.

We estimated CUE based on the stoichiometry of enzyme activity and elemental ratios in the microbial biomass[77]. The stoichiometric method has been found to be robust and correlated to substrate-non-specific ^{18}O labeling methods[78] and is useful because it is based on direct measurements of soil properties and can be more easily compared among studies[74]. We estimated CUE from ecological stoichiometry whereby CUE is a function of the difference between its elemental requirements for growth (C, N or P in biomass and enzymatic investment for acquisition) and the abundance of environmental substrate (C, N or P in soil organic matter). This approach assumes that enzyme activities scale with microbial production and organic matter concentration, and that microbial communities exhibit optimum resource allocation with respect to enzyme expression and environmental resources; these assumptions are empirically supported by Michaelis-Menten kinetics

and metabolic control analysis[77]. Based on this underlying assumption, CUE is therefore calculated as follows[77]:

$$CUE_{C:X} = CUE_{MAX}\left[\frac{S_{C:X}}{(S_{C:X} + K_X)}\right], \textbf{ where } S_{C:X} = \left(\frac{1}{EEA_{C:X}}\right)\left(\frac{B_{C:X}}{L_{C:X}}\right) \ (equation\ 4)$$

where $S_{C:X}$ is a scalar that represents the extent to which the allocation of enzyme activities offsets the disparity between the elemental composition of available resources and the composition of microbial biomass; K_x and CUE_{MAX} are constants: half-saturation constant (K_x) = 0.5; and the upper limit for microbial growth efficiency based on thermodynamic constraints, CUE_{MAX} = 0.6. EEA is extracellular enzyme activity (nmol g^{-1} h^{-1}); $EEA_{C:N}$ was calculated as BG/NAG, where BG = β-glucosidase and NAG = *N*-acetyl β-glucosaminidase; and $EEA_{C:P}$ was calculated as BG/P, where BG = β-glucosidase and P = phosphomonoesterase. Molar ratios of soil organic C : total N : total P were used as estimates of $L_{C:N}$ or $L_{C:P}$. Microbial biomass ($B_{C:X}$) C:N and C:P were also calculated as molar ratios.

Using the stoichiometric method, we found no change in CUE in this study (on 3°C and 8°C warming effects during the wet season; Extended Data Figure 6), or over 2-years following 3°C warming in surface soils[13]. However, given the apparent acceleration of enzyme activity via abiotic mechanisms (see discussion), we suggest that this renders low confidence in the stoichiometric method in this instance, given its assumption that enzymatic activity is correlated with biological synthesis[77].

Instantaneous temperature response of microbial growth and respiration. We used the instantaneous temperature response of microbial growth and respiration to: i) predict the effect of warming on *in situ* soil CO_2 emissions and ii) to determine the temperature adaptation of the bacterial community following two years of *in situ* warming. For the former, we measured the instantaneous temperature response of respiration and bacterial growth for control soils only. For the latter, we measured the instantaneous temperature response of bacterial community growth for all warming treatments and

controls; assuming the temperature adaptation of respiration responded similarly as for bacterial growth, as found in tropical soils elsewhere[20]. To determine the temperature response of bacteria growth, we used the leucine incorporation method[19]; for the temperature response of instantaneous respiration, we used incubation assays with measurement of headspace CO_2. Full details on these respective methods are described below.

The temperature response of bacterial community growth was determined by measuring instantaneous growth across a range of temperatures (4 to 40°C) using the leucine (Leu) incorporation method[79]. Soil (1 g dry weight) was mixed with 20 ml 17°C distilled water, vortexed for 3 min and centrifuged at 15°C for 10 min. The supernatant, with an extracted bacterial suspension, was transferred (1.5 ml) into microcentrifugation vials, which were pre-incubated in water baths for 0.5 to 1h before 2µl 3H-leucine (1-[4,5-3H] leucine, 37 MBq ml^{-1} and 5.74 TBq $mmol^{-1}$, Perkin-Elmer, USA) together with unlabelled Leu was added (resulting in 275 nM in the bacterial suspension). Trichloroacetic acid was added to terminate growth after 1 to 6.5h, depending on incubation temperature. Measurement of radioactivity was conducted following Bååth, et al. [79].

The instantaneous temperature response of respiration was determined by incubating 2 g fresh soil in 20 ml vials for 140 hours (at 10°C) or for 24 hours (at 28°C). At the end of each incubation, we sampled the vial headspace and determined the CO_2 concentration (using a GC equipped with a methanizer and a flame ionization detector) to calculate the respiration rate per g soil.

To estimate the degree of microbial community adaptation to temperature we used two complementary indices, the theoretical minimum temperature for growth (T_{min})[15] and the log ratio of activity at 40°C /4°C (temperature Sensitivity Index, SI)[80]. The T_{min} index provides insight on temperature adaptation across a broader temperature range and is calculated by the rate of increase in activity across temperatures from 4–28°C. The SI index provides alternative information on the

temperature adaptation of the bacterial community including also high temperatures. Because T_{min} and SI are closely related[19,81] we report both values but focus our analyses on the response of T_{min}.

Determination of T_{min} for respiration and growth and the predicted response of CO_2 efflux to in situ warming. The T_{min} of microbial activity was calculated using empirically defined microbial activity across the temperature range 4–28°C (where the increase in the SQRT of activity is linear), according to the Ratkowsky (square root) equation[15,17]:

$$\sqrt{Activity} = a * (T - T_{min})$$

where T is the measurement temperature, T_{min} is the minimum temperature for activity (temperature where activity = 0) and *a* is empirically defined by the slope parameter from the square root of activity plotted against temperature; and where activity is either bacterial or fungal growth rates, or respiration. We determined T_{min} for each field replicate (n = 5 plots).

We then used the instantaneous temperature sensitivity of bacterial activity (T_{min}) to model the CO_2 efflux response to warming, both with and without microbial community adaptation. To model the CO_2 efflux response to warming we used the following equation:

$$\text{Predicted } CO_2 = [a * (T - T_{min})]^2$$

where T_{min} is for control soils. To model the CO_2 efflux response to warming following temperature-adaptation of microbial communities, we refitted the model using the T_{min} determined for bacterial growth in experimentally warmed soils for two years by 3°C and 8°C ('adapted' communities).

Treatment effects on soil properties. To determine treatment effects on soil CO_2 emissions, soil moisture and temperature we used repeated measures ANOVA fitted by maximum likelihood (repeated measures model with time as random factor). To determine treatment effects (levels: control, +3°C and +8°C) on soil properties we used one-way ANOVA with post-hoc Tukey HSD tests. We used this approach for all soil properties, including enzyme V_{max} and the Q_{10} of V_{max} for each enzyme

550 determined at soil temperature. Prior to analyses all data were tested for normality using a Shapiro-
551 Wilk test and log-transformed where non-normally distributed.
552
553 ***Microbial community analysis.*** To determine temperature treatment effects on alpha diversity of soil
554 bacterial and fungal communities, we first applied general prevalence filtering using the R package
555 PERFect (PERmutation Filtering test for microbiome data)[82] (v0.2.4). Here we used the function
556 PERFect_sim with the alpha parameter set to 0.05 for the 16S rRNA data and 0.1 for the ITS data. We
557 also applied two complementary methods of prevalence filtering to determine how filtering influenced
558 alpha diversity estimates (see Supplementary Methods for complete details). We then calculated Hill
559 numbers using the R package hilldiv[83] (v1.5.1), specifically Observed richness (q-value = 0), Shannon
560 exponential (q-value = 1), and Simpson multiplicative inverse (q-value = 2). We used Shapiro-Wilk
561 Normality test and Bartlett's test of Homogeneity of Variances to determine whether Hill numbers
562 were normally distributed. In cases where both p-values were greater than 0.05 (parametric data), we
563 used ANOVA followed by Tukey post-hoc analysis to test for significance. For non-parametric data
564 (cases where one or both p-values were less than 0.05), we instead used Kruskal-Wallis followed by
565 Dunn test with Benjamini-Hochberg correction.
566
567 For soil bacterial and fungal beta diversity, we calculated distance matrices for the filtered data sets
568 using unweighted and weighted UniFrac[84] for the 16S rRNA data and Jensen-Shannon Divergence
569 and Bray-Curtis for the ITS data. To test for temperature treatment effects on beta diversity, we used
570 the vegan package[85] (v2.5-7) to first calculate beta dispersion for the distance matrices (betadisper
571 function), then perform a Permutation Test for Homogeneity of multivariate dispersions (permutest
572 function), and finally run PERMANOVA (adonis function; assuming equal dispersion) or Analysis of
573 Similarity (ANOSIM; where beta dispersion was significant).
574

To identify ASVs from the bacterial and fungal communities that were differentially abundant across temperature treatments, we used Indicator Species Analysis (ISA)[86] and linear discriminant analysis (LDA) effect size (LEfSe)[87]. Prior to differential abundance analysis, we applied PIME (Prevalence Interval for Microbiome Evaluation)[88] (v0.1.0) filtering to both complete datasets. PIME is a slightly more aggressive filtering tool specifically designed to work with data sets containing high variation among samples[88] — a pattern observed in the +8°C warming samples from the 16S rRNA data and all treatments from the ITS data (Extended Data Figs. 2c and 2f). PIME applies prevalence filtering on a per treatment basis and removes a substantial amount of within-group variation by eliminating low abundance ASVs in each treatment and retaining only those ASVs shared at the selected level of prevalence, within a given treatment[88]. Per the developer's recommendation, we first rarefied all samples to even depths (per sample: 16S rRNA = 25,088 reads, ITS = 9172 reads) and then split the data sets by predictor variable (temperature treatment) using the pime.split.by.variable function in R. Next, we calculated all prevalence intervals from 5% to 95% (increments of 5%) with the function pime.prevalence and then used the function pime.best.prevalence to choose the best prevalence. The best prevalence interval was selected when the out-of-bag (OOB) error rate first reached zero or close to zero. The most prevalent ASVs (at the best prevalence interval) were retained from each split. Splits were then merged to obtain the final, PIME filtered data set. ISA was computed with the R package *labdsv*[89] (v2.0-1)—ASVs were considered an indicator of a treatment if they had a p-value less than or equal to 0.05. LEfSe analysis was performed within the R package microbiomeMarker[90] (v0.0.1) using the following parameters: pre-sample normalization of the sum of values set to $1e^{+06}$, lda_cutoff = 2, kw_cutoff = 0.5, and wilcoxon_cutoff = 0.5. We used anvi'o[91] (v7-dev) to visualize the distribution of PIME-filtered 16S rRNA ASVs represented by more than 100 total reads and PIME-filtered ITS ASVs represented by more than 50 reads. We then overlaid the results of the ISA and LEfSe analyses. Hierarchical clustering of ASVs was performed using Euclidean distance and Ward

linkage against the ASV/sample abundance matrix while hierarchical clustering of samples was performed using Bray-Curtis distance and complete linkage.

To assess potential drivers of change in microbial community composition, we used three subsets of metadata to test correlations with community change; 1) environmental properties, 2) soil functional responses, and 3) temperature adaptive responses. For each of the three metadata subsets, we performed the following steps: i) use Shapiro-Wilk Normality Test to determine which metadata parameters are normally distributed; ii) use the R package bestNormalize[92] to find and execute the best normalization transformation for non-normally distributed parameters; iii) perform autocorrelation tests for all pair-wise comparisons; iv) remove autocorrelated parameters; v) run Mantel Tests to determine if any of the metadata subsets are significantly correlated with microbial community data; and vi) use the bioenv function (vegan package) to identify metadata parameters that are most strongly correlated with the community data. In last step, vii) we performed distance-based redundancy analysis (dbRDA) using capscale from the vegan package. First, we ran rankindex (vegan) to select the best community dissimilarity index. Then, we ran capscale for distance-based redundancy analysis. Next, we used envfit (vegan) to fit environmental parameters onto ordinations. And finally, we selected all metadata parameters that were significant for bioenv (see above) and/or envfit analyses for plotting the ordinations and vector overlays. For a detailed description of community analyses, including all references, see Supplementary Methods.

Data availability

Trimmed (primers removed) sequence data generated in this study are deposited in the European Nucleotide Archive (ENA) under Project Accession number PRJEB45074 (ERP129199), sample accession numbers ERS6485270–ERS6485284 (16S rRNA) and sample accession numbers ERS6485285– ERS6485299 (ITS). Raw fastq files can be accessed through the Smithsonian figshare,

at https://doi.org/10.25573/data.14686665 (16S rRNA) and https://doi.org/10.25573/data.14686755 (ITS). Related data and data products for individual analysis workflows are available through the Smithsonian figshare under the collection: https://doi.org/10.25573/data.c.5667571

Code availability

All code, reproducible workflows, and further information on data availability can be found on the project website at https://sweltr.github.io/high-temp/. The code embedded in the website is available on GitHub [https://github.com/sweltr/high-temp/] in R Markdown format. The version of code used in this study is archived under SWELTR Workflows v1.0 [https://github.com/sweltr/high-temp], DOI identifier, https://zenodo.org/badge/latestdoi/368915237

Acknowledgements | This study was supported by three fellowships to ATN, a UK NERC grant NE/T012226, a European Union Marie-Curie Fellowship FP7-2012-329360 and a STRI Tupper Fellowship. Further support came from a UK NERC grant NE/K01627X/1 to PM, an ANU Biology Innovation grant to PM and Simons Foundation grant No. 429440 to W. Wcislo, STRI, and support from the U.S. Department of Agriculture (USDA), Agricultural Research Service to KB. We thank Ben Turner for his contribution to SWELTR, especially during its initial phase of operation. For their support we further thank Oris Acevado, Dayana Agudo, Aleksandra Bielnicka, Gloria Broders, Melissa Cano, David Dominguez, Milton Garcia, Matthew Larsen, Julio Rodriguez, Hubert Szczygiel, Irene Torres, Esther Velasquez, William Wcislo, Klaus Winter and Joe Wright. Sequencing analyses were conducted on the Smithsonian High-Performance Cluster (SI/HPC), Smithsonian Institution (https://doi.org/10.25572/SIHPC). For the purpose of open access, the author has applied a Creative Commons Attribution (CC BY) licence to any Author Accepted Manuscript version arising from this submission.

Author Contributions Statement | ATN conceived the study. ATN, JJS, MM, JP, EB, KB and KS performed the study. ATN and JJS analysed the data. ATN wrote the paper with input from JJS, EB, KS, KB and PM.

Competing Interests Statement | The authors declare no competing interests. Mention of trade names or commercial products in this publication is solely for the purpose of providing specific information and does not imply recommendation or endorsement by the USDA. The USDA is an equal opportunity provider and employer. Reprints and permissions information is available at www.nature.com/reprints. Correspondence and requests for materials should be addressed to A.T.N. (A.Nottingham@leeds.ac.uk).

Figure Captions

Figure 1 | Microbial diversity decline and community change under 3°C and 8°C *in situ* soil warming in lowland tropical forest. Two years of soil warming caused significant decreases in (**a**) bacterial and (**b**) fungal diversity, determined by 16S rRNA and ITS sequencing, respectively. Data from the PIME filtered data sets for controls (blue), 3°C warming (green) and 8°C warming (red). Hierarchical clustering of ASVs (top dendrograms) based on Euclidean distance and Ward linkage. Hierarchical clustering of samples (right dendrograms) based on Bray-Curtis distance and complete linkage. Each vertical line in the main plot represents a unique ASV, where colour intensity indicates the log-normalized abundance, and no colour indicates an ASV that was either not detected or removed during prevalence filtering. The coloured bars below indicate ASVs that were enriched in different temperature treatments as determined by either Indicator Species Analysis (IndVal) or Linear discriminant analysis Effect Size (LEfSe). Additional data for each sample are presented in the plots on the right. Diversity estimates charts show the total number of reads, observed richness, Shannon exponential index, and Inverse Simpson index. Taxonomic profiles show the proportion of major classes (16S rRNA data) or orders (ITS data). All analyses are for soil samples collected from n = 5 independent experimental plots, for each treatment level.

Figure 2 | The response of microbial growth and enzyme activity to 3°C and 8°C soil warming, and the relationship between the temperature response of growth and activity with microbial community changes. (**a–b**) Microbial growth was determined for bacteria for each treatment using Leu-incorporation incubation assays across a temperature range of 4–40ºC. The minimum temperature for growth (T_{min}) increased with warming (see **b,** where $P = 0.006$ for +8°C treatment), but growth declined at high temperatures (>30–34°C; see lighter shaded points in (**a**); these data were not used for the linear model to determine T_{min}). **(c)** Activities were determined for 10 enzymes (ß-xylanase shown here, six others responded similarly; see SI) across an incubation temperature range of 4–40°C. The maximum potential activity—at soil temperature per unit microbial C—increased with warming for 7 out of 10 enzymes (see **d**) and increased across high temperature ranges (to 40°C) illustrating a decoupling of growth and activity above 30°C. (**e**) The microbial community composition change was related to the temperature response of growth (T_{min}) and of enzyme activities (Q_{10} of V_{max}) for **i**) bacteria and **ii**) fungi. Bacterial growth and enzyme activity are plotted using a linear transformation (square root). Microbial community composition change estimated using Distance-based Redundancy Analysis (db-RDA) based on Bray-Curtis dissimilarity; see Extended Data (Table 2, Fig. 5) for relationships between community composition change and other soil properties. For scatter plots (**a**, **c**) the error bars represent mean ± one standard error, for n = 5 plots. Fitted lines depict linear functions with 95% confidence intervals shown. For box plots (**b**, **d**), the centre line of each box plot represents the median, the lower and upper hinges represent the first and third quartiles and whiskers represent + 1.5 the interquartile range. Statistical differences are shown where ** $P < 0.05$, ** $P < 0.01$ (by ANOVA); where shown in **b**, $P = 0.006$; in **d**, $P = 0.016$. All analyses are for soil samples collected from n = 5 independent experimental plots, for each treatment level.

Figure 3 | The response of soil CO_2 efflux to *in situ* warming by 3°C to 8°C is greater than the increase predicted by the temperature response of microbial respiration and growth. (a). Data points are measurements of soil CO_2 efflux from control (blue), 3°C warming (green) and 8°C warming (red). The response of CO_2 emission to temperature was described by a square root function ('Observed' line; $CO_2 = 1.9 \times T^2 - 45$; $R^2 = 0.68$, $P < 0.001$, F = 556). The modelled CO_2 efflux responses ('Predicted' lines) are based on measured T_{min} at ambient temperature (blue dash line = no adaptation; $CO_2 = 1.21 \times T^2 - 0.17$; $R^2 = 0.87$, $P < 0.001$, F = 124) and T_{min} change after two years of warming indicating community adaptation (green dash line = 3°C adaptation, $CO_2 = 1.24 \times T^2 - 0.18$; $R^2 = 0.87$, $P < 0.001$, F = 118; and red dash line = 8°C adaptation, $CO_2 = 1.25 \times T^2 - 0.20$; $R^2 = 0.86$, $P < 0.001$, F = 111). Lines depict square root functions with 95% confidence intervals shown. The box plots show the treatment effects on (**b**) soil CO_2 efflux and (**c**) soil temperature (repeated measures ANOVA; ** $P < 0.01$; *** $P < 0.001$; where treatment effects on soil CO_2 efflux were $P = 0.00392$ and $P < 0.001$ for 3°C and 8°C warming, respectively). The soil temperature and soil CO_2 efflux by treatment was, for controls: 26 ± 1 °C and 4.74 ± 0.25 µmol CO_2 m^{-2} s^{-1}, 3°C warming: 29 ± 2°C and 8.42 ± 0.44 µmol CO_2 m^{-2} s^{-1}, 8°C warming: 34 ± 7°C and 15.98 ± 1.68 µmol CO_2 m^{-2} s^{-1} (mean ± one standard error, n = 5

plots). The centre line of each box plot represents the median, the lower and upper hinges represent the first and third quartiles and whiskers represent + 1.5 the interquartile range; the dashed lines represent means. All analyses are for soil samples collected from n = 5 independent experimental plots, for each treatment level.

References

1 Cavicchioli, R. *et al.* Scientists' warning to humanity: microorganisms and climate change. *Nature Reviews Microbiology* **17**, 569-586, doi:10.1038/s41579-019-0222-5 (2019).

2 Jackson, R. B. *et al.* The ecology of soil carbon: pools, vulnerabilities, and biotic and abiotic controls. *Annual Review of Ecology, Evolution, and Systematics* **48**, 419-445, doi:10.1146/annurev-ecolsys-112414-054234 (2017).

3 Pan, Y. *et al.* A large and persistent carbon sink in the world's forests. *Science* **333**, 988-993, doi:10.1126/science.1201609 (2011).

4 Myers, N., Mittermeier, R. A., Mittermeier, C. G., da Fonseca, G. A. B. & Kent, J. Biodiversity hotspots for conservation priorities. *Nature* **403**, 853-858, doi:10.1038/35002501 (2000).

5 IPCC. *Climate Change 2021: The Physical Science Basis. Contribution of Working Group I to the Sixth Assessment Report of the Intergovernmental Panel on Climate Change*. (Cambridge University Press, 2021).

6 Mora, C. *et al.* The projected timing of climate departure from recent variability. *Nature* **502**, 183, doi:0.1038/Nature12540 (2013).

7 Wood, T. E. *et al.* in *Ecosystem Consequences of Soil Warming: Microbes, Vegetation, Fauna and Soil Biogeochemistry* (ed J. Mohan) Ch. 14, 385-439 (Academic Press, 2019).

8 Davidson, E. A. & Janssens, I. A. Temperature sensitivity of soil carbon decomposition and feedbacks to climate change. *Nature* **440**, 165-173, doi:10.1038/nature04514 (2006).

9 van Gestel, N. *et al.* Predicting soil carbon loss with warming. *Nature* **554**, E4-E5, doi:10.1038/nature20150 (2018).

10 Melillo, J. M. *et al.* Long-term pattern and magnitude of soil carbon feedback to the climate system in a warming world. *Science* **358**, 101-104, doi:10.1126/science.aan2874 (2017).

11 Romero-Olivares, A. L., Allison, S. D. & Treseder, K. K. Soil microbes and their response to experimental warming over time: A meta-analysis of field studies. *Soil Biol Biochem* **107**, 32-40, doi:10.1016/j.soilbio.2016.12.026 (2017).

12 Anderson-Teixeira, K. J., Wang, M. M. H., McGarvey, J. C. & LeBauer, D. S. Carbon dynamics of mature and regrowth tropical forests derived from a pantropical database (TropForC-db). *Global Change Biol* **22**, 1690-1709, doi:10.1111/gcb.13226 (2016).

13 Nottingham, A. T., Meir, P., Velasquez, E. & Turner, B. L. Soil carbon loss by experimental warming in a tropical forest. *Nature* **584**, 234-237, doi:10.1038/s41586-020-2566-4 (2020).

14 DeAngelis, K. M. *et al.* Long-term forest soil warming alters microbial communities in temperate forest soils. *Front Microbiol* **6**, doi:ARTN 10410.3389/fmicb.2015.00104 (2015).

15 Bååth, E. Temperature sensitivity of soil microbial activity modeled by the square root equation as a unifying model to differentiate between direct temperature effects and microbial community adaptation. *Global Change Biol* **24**, 2850-2861, doi:10.1111/gcb.14285 (2018).

16 Wieder, W. R., Bonan, G. B. & Allison, S. D. Global soil carbon projections are improved by modelling microbial processes. *Nat Clim Change* **3**, 909-912, doi:10.1038/Nclimate1951 (2013).

17 Ratkowsky, D. A., Olley, J., Mcmeekin, T. A. & Ball, A. Relationship between temperature and growth-rate of bacterial cultures. *J Bacteriol* **149**, 1-5 (1982).
18 Rinnan, R., Rousk, J., Yergeau, E., Kowalchuk, G. A. & Bååth, E. Temperature adaptation of soil bacterial communities along an Antarctic climate gradient: predicting responses to climate warming. *Global Change Biol* **15**, 2615-2625, doi:10.1111/j.1365-2486.2009.01959.x (2009).
19 Nottingham, A. T., Bååth, E., Reischke, S., Salinas, N. & Meir, P. Adaptation of soil microbial growth to temperature: using a tropical elevation gradient to predict future changes. *Global Change Biol*, doi:10.1111/gcb.14502 (2019).
20 Li, J. Q., Bååth, E., Pei, J. M., Fang, C. M. & Nie, M. Temperature adaptation of soil microbial respiration in alpine, boreal and tropical soils: An application of the square root (Ratkowsky) model. *Global Change Biol* **27**, 1281-1292, doi:10.1111/gcb.15476 (2021).
21 Rousk, J., Frey, S. D. & Bååth, E. Temperature adaptation of bacterial communities in experimentally warmed forest soils. *Global Change Biol* **18**, 3252-3258, doi:10.1111/j.1365-2486.2012.02764.x (2012).
22 Nottingham, A. T. *et al.* Annual to decadal temperature adaptation of the soil bacterial community after translocation across an elevation gradient in the Andes. *Soil Biology and Biochemistry* **158**, 108217, doi:/10.1016/j.soilbio.2021.108217 (2021).
23 Nottingham, A. T. *et al.* Microbial responses to warming enhance soil carbon loss following translocation across a tropical forest elevation gradient. *Ecol Lett* **22**, 1889-1899, doi:10.1111/ele.13379 (2019).
24 Donhauser, J., Niklaus, P. A., Rousk, J., Larose, C. & Frey, B. Temperatures beyond the community optimum promote the dominance of heat-adapted, fast growing and stress resistant bacteria in alpine soils. *Soil Biology and Biochemistry* **148**, 107873, doi:10.1016/j.soilbio.2020.107873 (2020).
25 Mangan, S. A. *et al.* Negative plant-soil feedback predicts tree-species relative abundance in a tropical forest. *Nature* **466**, 752-755, doi:10.1038/nature09273 (2010).
26 Pold, G., Melillo, J. M. & DeAngelis, K. M. Two decades of warming increases diversity of a potentially lignolytic bacterial community. *Front Microbiol* **6**, doi:ARTN 48010.3389/fmicb.2015.00480 (2015).
27 Zhou, J. Z. *et al.* Temperature mediates continental-scale diversity of microbes in forest soils. *Nat Commun* **7**, doi:ARTN 1208310.1038/ncomms12083 (2016).
28 Tedersoo, L. *et al.* Global diversity and geography of soil fungi. *Science* **346**, 1078 (2014).
29 Oliverio, A. M., Bradford, M. A. & Fierer, N. Identifying the microbial taxa that consistently respond to soil warming across time and space. *Global Change Biol* **23**, 2117-2129, doi:10.1111/gcb.13557 (2017).
30 Bahram, M. *et al.* Structure and function of the global topsoil microbiome. *Nature* **560**, 233-237, doi:10.1038/s41586-018-0386-6 (2018).
31 Spracklen, D. V., Baker, J. C. A., Garcia-Carreras, L. & Marsham, J. H. The effects of tropical vegetation on rainfall. *Annu Rev Env Resour* **43**, 193-218, doi:10.1146/annurev-environ-102017-030136 (2018).
32 Bradford, M. A. Thermal adaptation of decomposer communities in warming soils. *Front Microbiol* **4**, doi:10.3389/Fmicb.2013.00333 (2013).
33 Pietikäinen, J., Pettersson, M. & Bååth, E. Comparison of temperature effects on soil respiration and bacterial and fungal growth rates. *FEMS Microbiol Ecol* **52**, 49-58, doi:10.1016/j.femsec.2004.10.002 (2005).
34 Mori, A. S. *et al.* Biodiversity–productivity relationships are key to nature-based climate solutions. *Nat Clim Change* **11**, 543-550, doi:10.1038/s41558-021-01062-1 (2021).
35 Delgado-Baquerizo, M. *et al.* Multiple elements of soil biodiversity drive ecosystem functions across biomes. *Nat Ecol Evol* **4**, 210-220, doi:10.1038/s41559-019-1084-y (2020).

36 Wagg, C., Bender, S. F., Widmer, F. & van der Heijden, M. G. A. Soil biodiversity and soil community composition determine ecosystem multifunctionality. *P Natl Acad Sci USA* **111**, 5266-5270, doi:10.1073/pnas.1320054111 (2014).

37 Nottingham, A. T. *et al.* Microbes follow Humboldt: temperature drives plant and soil microbial diversity patterns from the Amazon to the Andes. *Ecology* **99**, 2455-2466, doi:10.1002/ecy.2482 (2018).

38 Brown, J. H., Gillooly, J. F., Allen, A. P., Savage, V. M. & West, G. B. Toward a metabolic theory of ecology. *Ecology* **85**, 1771-1789, doi:10.1890/03-9000 (2004).

39 Brown, J. H. Why are there so many species in the tropics? *J Biogeogr* **41**, 8-22, doi:10.1111/jbi.12228 (2014).

40 LaManna, J. A. *et al.* Plant diversity increases with the strength of negative density dependence at the global scale. *Science* **356**, 1389-1392, doi:10.1126/science.aam5678 (2017).

41 Bagchi, R. *et al.* Pathogens and insect herbivores drive rainforest plant diversity and composition. *Nature* **506**, 85-88, doi:10.1038/nature12911 (2014).

42 Lapebie, P., Lombard, V., Drula, E., Terrapon, N. & Henrissat, B. Bacteroidetes use thousands of enzyme combinations to break down glycans. *Nat Commun* **10**, doi:10.1038/s41467-019-10068-5 (2019).

43 Makhalanyane, T. P. *et al.* Microbial ecology of hot desert edaphic systems. *Fems Microbiol Rev* **39**, 203-221, doi:10.1093/femsre/fuu011 (2015).

44 Aydogan, E. L., Moser, G., Muller, C., Kampfer, P. & Glaeser, S. P. Long-Term Warming Shifts the Composition of Bacterial Communities in the Phyllosphere of Galium album in a Permanent Grassland Field-Experiment. *Front Microbiol* **9**, doi:10.3389/fmicb.2018.00144 (2018).

45 Hu, D. Y., Zang, Y., Mao, Y. J. & Gao, B. L. Identification of Molecular Markers That Are Specific to the Class Thermoleophilia. *Front Microbiol* **10**, doi:10.3389/fmicb.2019.01185 (2019).

46 Mohan, J. E. *et al.* Mycorrhizal fungi mediation of terrestrial ecosystem responses to global change: mini-review. *Fungal Ecol* **10**, 3-19, doi:10.1016/j.funeco.2014.01.005 (2014).

47 Manzoni, S., Taylor, P., Richter, A., Porporato, A. & Agren, G. I. Environmental and stoichiometric controls on microbial carbon-use efficiency in soils. *New Phytol* **196**, 79-91, doi:10.1111/j.1469-8137.2012.04225.x (2012).

48 Allison, S. D., Wallenstein, M. D. & Bradford, M. A. Soil-carbon response to warming dependent on microbial physiology. *Nat Geosci* **3**, 336-340, doi:10.1038/Ngeo846 (2010).

49 Reed, S. C. *et al.* Soil biogeochemical responses of a tropical forest to warming and hurricane disturbance. *Advances in Ecological Research* **62**, 225– 252 (2020).

50 Nottingham, A. T., Turner, B. L., Stott, A. W. & Tanner, E. V. J. Nitrogen and phosphorus constrain labile and stable carbon turnover in lowland tropical forest soils. *Soil Biol Biochem* **80**, 26-33, doi:10.1016/J.Soilbio.2014.09.012 (2015).

51 Walker, T. W. N. *et al.* Microbial temperature sensitivity and biomass change explain soil carbon loss with warming. *Nat Clim Change* **8**, 885, doi:10.1038/s41558-018-0259-x (2018).

52 Kemmitt, S. J. *et al.* Mineralization of native soil organic matter is not regulated by the size, activity or composition of the soil microbial biomass—a new perspective. *Soil Biology and Biochemistry* **40**, 61-73, doi:10.1016/j.soilbio.2007.06.021 (2008).

53 Nannipieri, P., Trasar-Cepeda, C. & Dick, R. P. Soil enzyme activity: a brief history and biochemistry as a basis for appropriate interpretations and meta-analysis. *Biol Fert Soils* **54**, 11-19, doi:10.1007/s00374-017-1245-6 (2018).

54 Wallenstein, M., Allison, S., Ernakovich, J., Steinweg, J. M. & Sinsabaugh, R. in *Soil Enzymology* Vol. 22 *Soil Biology* (eds Girish Shukla & Ajit Varma) Ch. 13, 245-258 (Springer Berlin Heidelberg, 2011).

55 Zhou, X. Y., Chen, L., Xu, J. M. & Brookes, P. C. Soil biochemical properties and bacteria community in a repeatedly fumigated-incubated soil. *Biol Fert Soils* **56**, 619-631, doi:10.1007/s00374-020-01437-0 (2020).

56 Sanchez-Julia, M. & Turner, B. L. Abiotic contribution to phenol oxidase activity across a manganese gradient in tropical forest soils. *Biogeochemistry*, doi:10.1007/s10533-021-00764-0 (2021).

57 Razavi, B. S., Liu, S. B. & Kuzyakov, Y. Hot experience for cold-adapted microorganisms: Temperature sensitivity of soil enzymes. *Soil Biol Biochem* **105**, 236-243, doi:10.1016/j.soilbio.2016.11.026 (2017).

58 Pinney, M. M. *et al.* Parallel molecular mechanisms for enzyme temperature adaptation. *Science* **371**, eaay2784, doi:10.1126/science.aay2784 (2021).

59 Fanin, N. *et al.* Soil enzymes in response to climate warming: Mechanisms and feedbacks. *Funct Ecol*, doi:10.1111/1365-2435.14027 (2022).

60 Hall, S. J. & Silver, W. L. Iron oxidation stimulates organic matter decomposition in humid tropical forest soils. *Global Change Biol* **19**, 2804-2813, doi:10.1111/gcb.12229 (2013).

61 Freeman, C., Ostle, N. & Kang, H. An enzymic 'latch' on a global carbon store. *Nature* **409**, 149 (2001).

62 Sarmiento, C. *et al.* Soilborne fungi have host affinity and host-specific effects on seed germination and survival in a lowland tropical forest. *P Natl Acad Sci USA* **114**, 11458-11463, doi:10.1073/pnas.1706324114 (2017).

63 Condit, R., Perez, R., Lao, S., Aguilar, S. & Hubbell, S. P. Demographic trends and climate over 35 years in the Barro Colorado 50 ha plot. *For Ecosyst* **4**, doi:10.1186/s40663-017-0103-1 (2017).

64 Woodring, W. P. Geology of Barro Colorado Island. *Smithsonian Miscellaneous Collections* **135**, 1 – 39 (1958).

65 Sanchez, P. A. & Logan, T. J. Myths and Science About the Chemistry and Fertility of Soils in the Tropics. *Sssa Spec Publ* **29**, 35-46 (1992).

66 Callahan, B. J. *et al.* DADA2: High-resolution sample inference from Illumina amplicon data. *Nat Methods* **13**, 581-583, doi:10.1038/nmeth.3869 (2016).

67 Brookes, P. C., Landman, A., Pruden, G. & Jenkinson, D. S. Chloroform fumigation and the release of soil-nitrogen - a rapid direct extraction method to measure microbial biomass nitrogen in soil. *Soil Biol Biochem* **17**, 837-842, doi:10.1016/0038-0717(85)90144-0 (1985).

68 Vance, E. D., Brookes, P. C. & Jenkinson, D. S. An extraction method for measuring soil microbial biomass-C. *Soil Biol Biochem* **19**, 703-707 (1987).

69 Jenkinson, D. S., Brookes, P. C. & Powlson, D. S. Measuring soil microbial biomass. *Soil Biol Biochem* **36**, 5-7, doi:10.1016/j.soilbio.2003.10.002 (2004).

70 Kouno, K., Tuchiya, Y. & Ando, T. Measurement of soil microbial biomass phosphorus by an anion-exchange membrane method. *Soil Biol Biochem* **27**, 1353-1357 (1995).

71 Tabatabai, M. A. in *Methods of soil analysis. Part 2. Microbiological and biochemical properties.* (eds R. Weaver *et al.*) 778-833 (SSSA, 1994).

72 Marx, M. C., Wood, M. & Jarvis, S. C. A microplate fluorimetric assay for the study of enzyme diversity in soils. *Soil Biol Biochem* **33**, 1633-1640 (2001).

73 Price, N., Stevens, L. *Fundamentals of Enzymology: Cell and Molecular Biology of Catalytic Proteins*. (Oxford University Press, 1999).

74 Hagerty, S. B., Allison, S. D. & Schimel, J. P. Evaluating soil microbial carbon use efficiency explicitly as a function of cellular processes: implications for measurements and models. *Biogeochemistry* **140**, 269-283, doi:10.1007/s10533-018-0489-z (2018).

75 Frey, S. D., Lee, J., Melillo, J. M. & Six, J. The temperature response of soil microbial efficiency and its feedback to climate. *Nat Clim Change* **3**, 395-398, doi:10.1038/Nclimate1796 (2013).

76 Spohn, M. *et al.* Soil microbial carbon use efficiency and biomass turnover in a long-term fertilization experiment in a temperate grassland. *Soil Biol Biochem* **97**, 168-175, doi:10.1016/j.soilbio.2016.03.008 (2016).
77 Sinsabaugh, R. L. *et al.* Stoichiometry of microbial carbon use efficiency in soils. *Ecological Monographs* **86**, 172-189, doi:10.1890/15-2110.1 (2016).
78 Geyer, K. M., Dijkstra, P., Sinsabaugh, R. & Frey, S. D. Clarifying the interpretation of carbon use efficiency in soil through methods comparison. *Soil Biol Biochem* **128**, 79-88, doi:10.1016/j.soilbio.2018.09.036 (2019).
79 Bååth, E., Pettersson, M. & Söderberg, K. H. Adaptation of a rapid and economical microcentrifugation method to measure thymidine and leucine incorporation by soil bacteria. *Soil Biol Biochem* **33**, 1571-1574, doi:10.1016/S0038-0717(01)00073-6 (2001).
80 Bárcenas-Moreno, G., Gomez-Brandon, M., Rousk, J. & Bååth, E. Adaptation of soil microbial communities to temperature: comparison of fungi and bacteria in a laboratory experiment. *Global Change Biol* **15**, 2950-2957, doi:10.1111/j.1365-2486.2009.01882.x (2009).
81 Rinnan, R., Rousk, J., Yergeau, E., Kowalchuk, G. A. & Bååth, E. Temperature adaptation of soil bacterial communities along an Antarctic climate gradient: predicting responses to climate warming. *Global Change Biol* **15**, 2615-2625, doi:10.1111/j.1365-2486.2009.01959.x (2009).
82 Smirnova, E., Huzurbazar, S. & Jafari, F. PERFect: PERmutation Filtering test for microbiome data. *Biostatistics* **20**, 615-631, doi:10.1093/biostatistics/kxy020 (2019).
83 Alberdi, A. & Gilbert, M. T. P. hilldiv: an R package for the integral analysis of diversity based on Hill numbers. *bioRxiv*, 545665, doi:10.1101/545665 (2019).
84 Lozupone, C., Lladser, M. E., Knights, D., Stombaugh, J. & Knight, R. UniFrac: an effective distance metric for microbial community comparison. *ISME J* **5**, 169-172, doi:10.1038/ismej.2010.133 (2011).
85 Vegan: Community Ecology Package (R Package Version 2 (0), 2012).
86 Dufrene, M. & Legendre, P. Species assemblages and indicator species: The need for a flexible asymmetrical approach. *Ecological Monographs* **67**, 345-366, doi:10.1890/0012-9615(1997)067[0345:Saaist]2.0.Co;2 (1997).
87 Segata, N. *et al.* Metagenomic biomarker discovery and explanation. *Genome Biol* **12**, doi:10.1186/gb-2011-12-6-r60 (2011).
88 Roesch, L. F. W. *et al.* pime: A package for discovery of novel differences among microbial communities. *Mol Ecol Resour* **20**, 415-428, doi:10.1111/1755-0998.13116 (2020).
89 labdsv: Ordination and multivariate analysis for ecology (R package, 2017).
90 microbiomeMarker: microbiome biomarker analysis (2020).
91 Eren, A. M. *et al.* Anvi'o: an advanced analysis and visualization platform for 'omics data. *Peerj* **3**, e1319, doi:10.7717/peerj.1319 (2015).
92 Peterson, R. A. & Cavanaugh, J. E. Ordered quantile normalization: a semiparametric transformation built for the cross-validation era. *J Appl Stat* **47**, 2312-2327, doi:10.1080/02664763.2019.1630372 (2020).

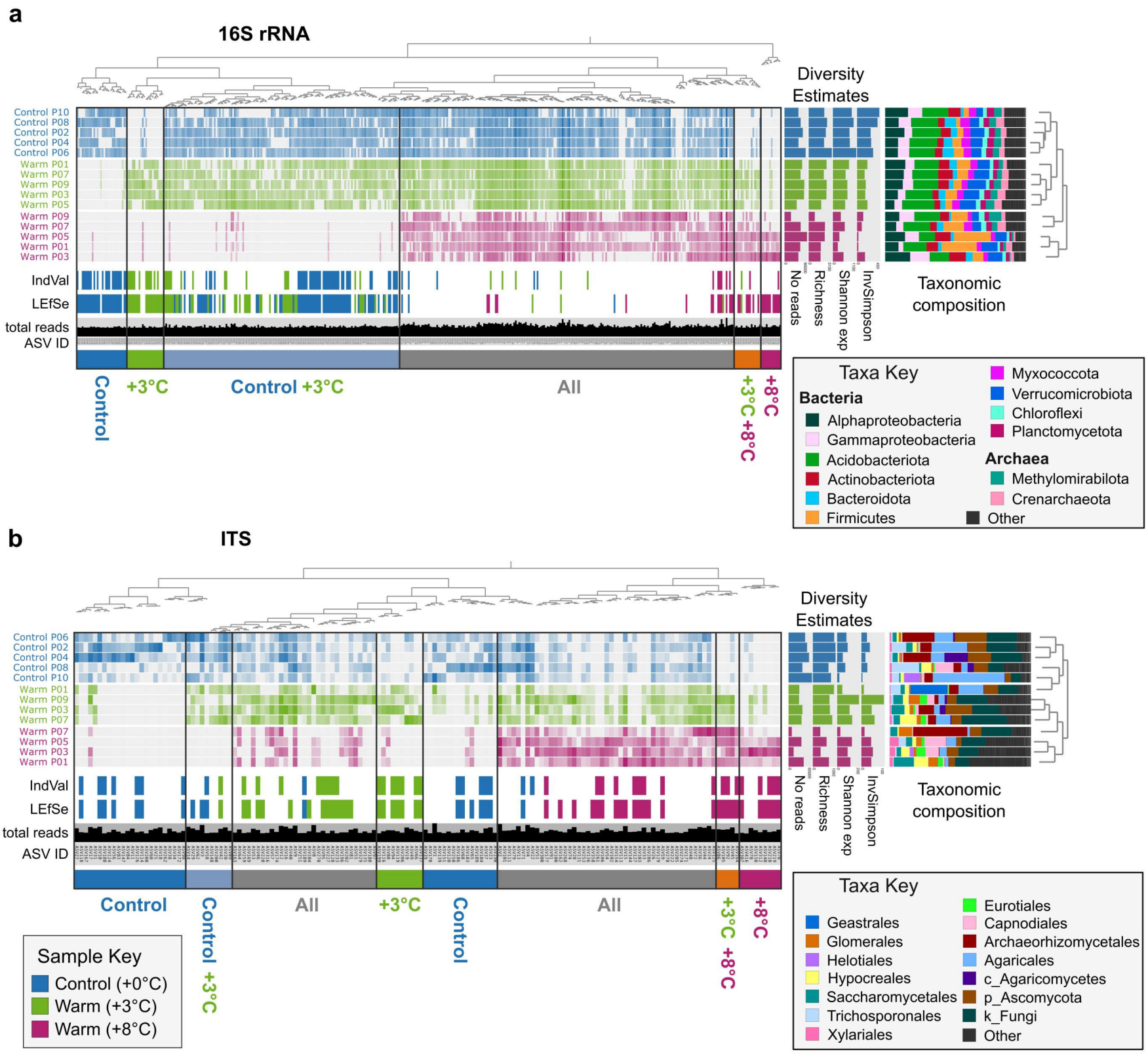
a
16S rRNA
Diversity Estimates
Control P10
Control P08
Control P02
Control P04
Control P06
Warm P01
Warm P07
Warm P09
Warm P03
Warm P05
Warm P09
Warm P07
Warm P05
Warm P01
Warm P03
IndVal
LEfSe
total reads
ASV ID
No reads
Richness
Shannon exp
InvSimpson
Taxonomic composition
Control
+3°C
Control +3°C
All
+3°C +8°C
+8°C
Taxa Key
Bacteria
Alphaproteobacteria
Gammaproteobacteria
Acidobacteriota
Actinobacteriota
Bacteroidota
Firmicutes
Myxococcota
Verrucomicrobiota
Chloroflexi
Planctomycetota
Archaea
Methylomirabilota
Crenarchaeota
Other
b
ITS
Diversity Estimates
Control P06
Control P02
Control P04
Control P08
Control P10
Warm P01
Warm P09
Warm P03
Warm P07
Warm P07
Warm P05
Warm P03
Warm P01
IndVal
LEfSe
total reads
ASV ID
No reads
Richness
Shannon exp
InvSimpson
Taxonomic composition
Control
Control +3°C
All
+3°C
Control
All
+3°C +8°C
+8°C
Sample Key
Control (+0°C)
Warm (+3°C)
Warm (+8°C)
Taxa Key
Geastrales
Glomerales
Helotiales
Hypocreales
Saccharomycetales
Trichosporonales
Xylariales
Eurotiales
Capnodiales
Archaeorhizomycetales
Agaricales
c_Agaricomycetes
p_Ascomycota
k_Fungi
Other

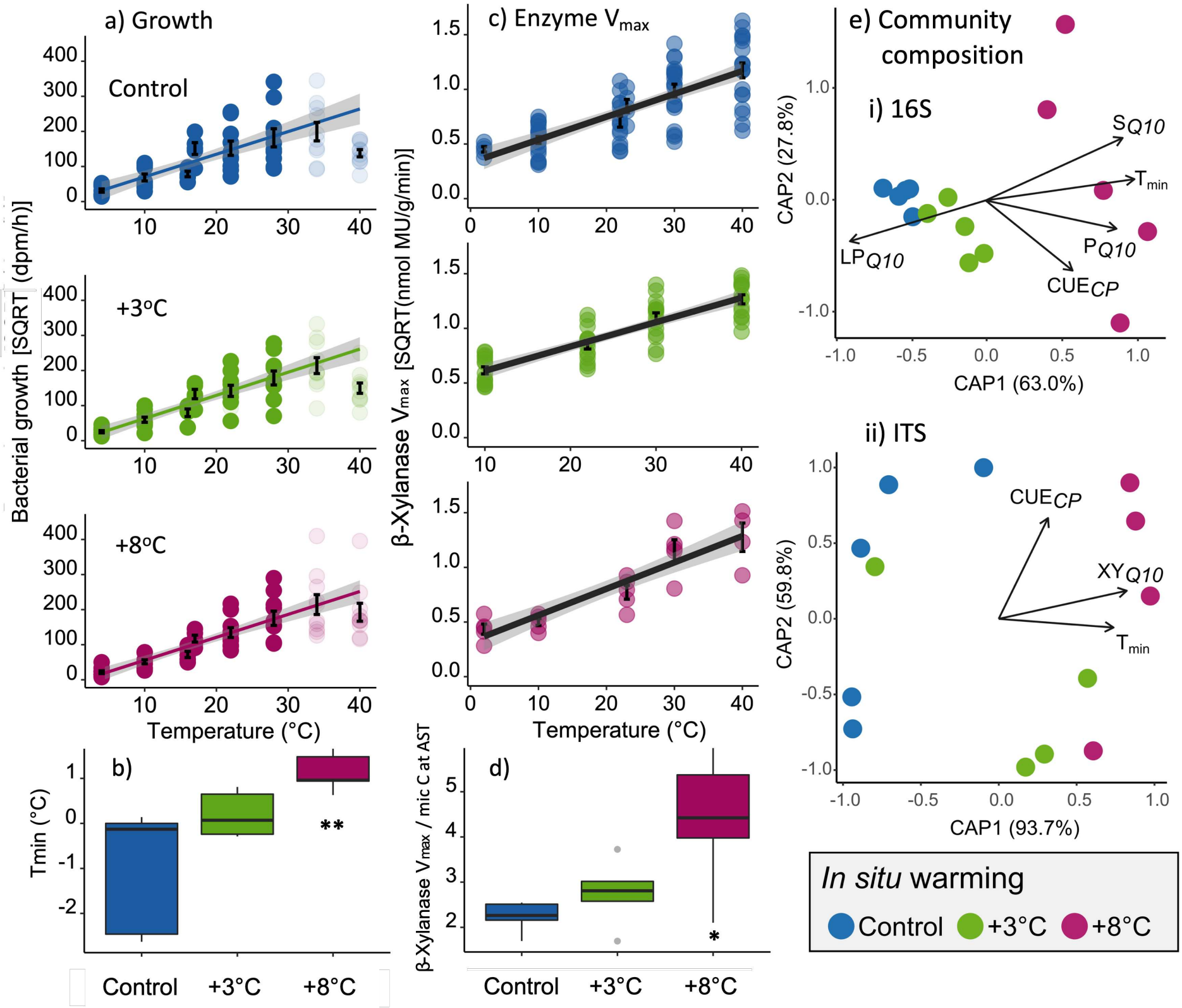
a) Growth
Control
+3°C
+8°C
Bacterial growth [SQRT (dpm/h)]
Temperature (°C)
c) Enzyme V_{max}
β-Xylanase V_{max} [SQRT(nmol MU/g/min)]
Temperature (°C)
e) Community composition
i) 16S
S_{Q10}
T_{min}
P_{Q10}
CUE_{CP}
LP_{Q10}
CAP2 (27.8%)
CAP1 (63.0%)
ii) ITS
CUE_{CP}
XY_{Q10}
T_{min}
CAP2 (59.8%)
CAP1 (93.7%)
b)
Tmin (°C)
**
Control
+3°C
+8°C
d)
β-Xylanase V_{max} / mic C at AST
*
Control
+3°C
+8°C
In situ warming
Control
+3°C
+8°C

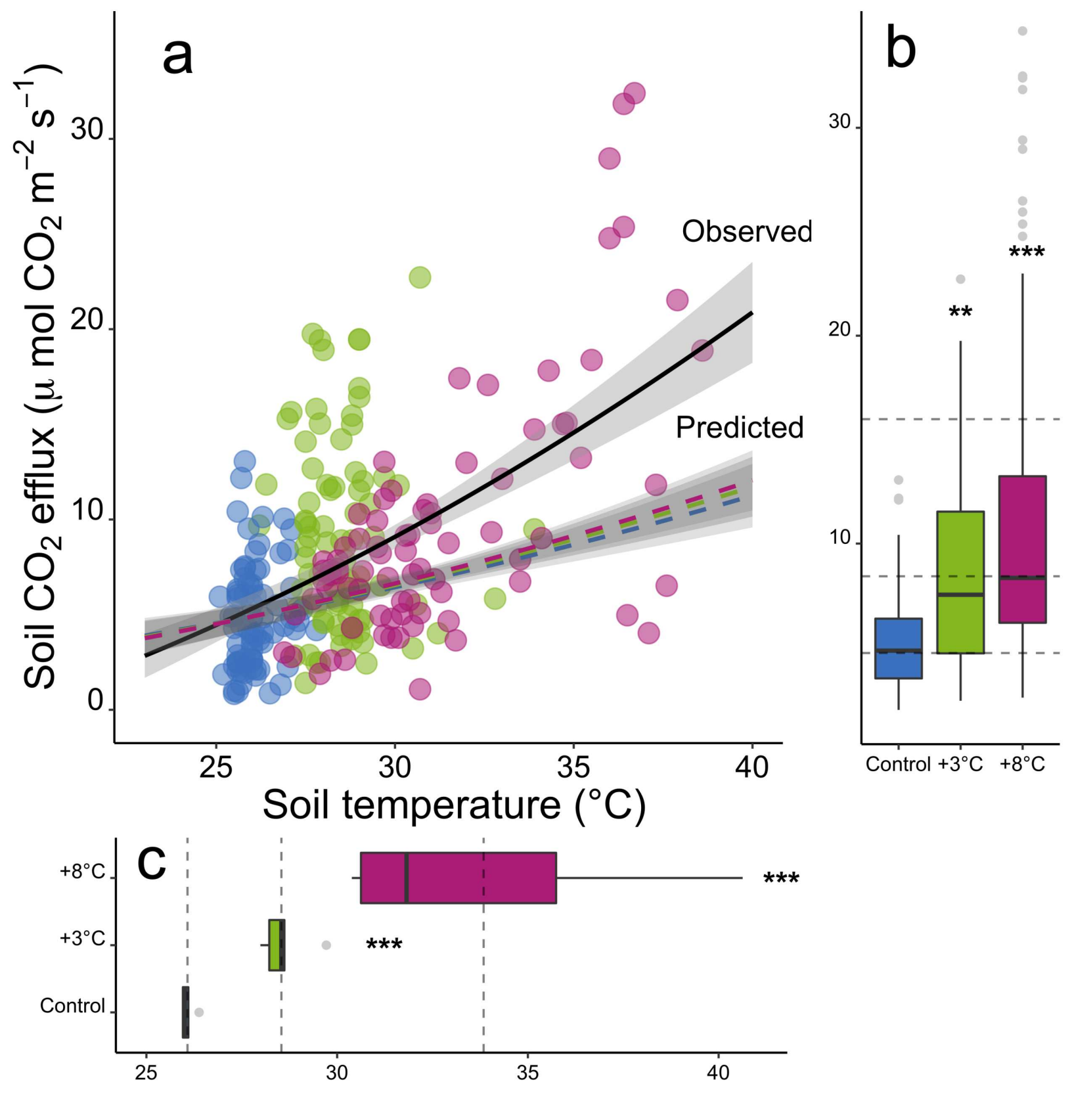
a
Soil CO2 efflux (μ mol CO2 m−2 s−1)
Observed
Predicted
Soil temperature (°C)
b
Control
+3°C
+8°C
**
***
c
+8°C
+3°C
Control
***
***